ISSN: 2277-9655
(I2OR), Publication Impact Factor: 3.785

IJESRT

INTERNATIONAL JOURNAL OF ENGINEERING SCIENCES & RESEARCH TECHNOLOGY

EFFECT OF POROSITY IN SUBSTITUTE BIRD UNDER HIGH VELOCITY LOADING

Sd. Abdul Kalam*, R Vijaya Kumar, G Ranga Janardhana

*Assistant Professor, PVP Siddhartha Institute of Technology, Kanuru, Vijayawada, India.
Manager in R & D, Hindustan Aeronautics Limited, Bangalore, India.
Professor & Director of IST, Jawaharlal Nehru Technological University Kakinada, India.

ABSTRACT

Impact events involving laminate composites had been largely studied through computational approaches, due to mainly to the technical difficulties and high costs associated with experimental tests, and the availability of highly sophisticated computational codes. The impact constraints are active only on the contact / target interface, so energy conservation is enforced only for contact elements. The underlying finite elements defining the interior of impacting bodies do not satisfy energy conservation. In the present work, high velocity impact event of 'dummy bird' against balanced Epoxy_Carbon_UD laminate composite structure was simulated through AUTODYNE explicit finite element package. Smoothed particle hydrodynamics (SPH) techniques is adopted to describe the motion of the impacted composite plate and the soft body projectile, with different porosities. The obtained energy and momentum variations with time from different porosities of two bird models are compared and results were plotted.

KEYWORDS: Impact, Laminate composite, FEM, Birds, Modeling, SPH, Hydrodynamic theory.

INTRODUCTION

Impact of bird on aircrafts has been one of the most dangerous risks to the safety of space vehicles. Although most bird strike event involves relatively small birds, which doesn't cause the catastrophic consequences, the possibility of severe damage generated by impacts with larger birds cannot be neglected. In order to ensure tolerance to bird strike damage, aircraft structures have to fulfill the airworthiness specifications prescribed by FAA or JAA.

As per certification process, an aircraft must demonstrate its ability to land safely after being struck by a bird anywhere on the structure, at normal operating speeds [1]. Although substantial and costly damage may occur, the performance of the key components, including the wing, cowling and engines, must be demonstrated. Impacted components must maintain structural integrity during the large transient loading resulting from bird strike loads. Past experience has been to demonstrate this compliance through full-scale tests. Because of the costs and time involved, there is a need to improve modeling capabilities and enable verification by numerical methods. This in turn will help to decrease the number of destructive testing required. To accurately predict the response of an aircraft structure under impact loading, it is essential to have an accurate bird model.

Energy conservation is relatively easy to satisfy for rigid impact (when both contact and target surfaces are rigid) as compared to flexible impact (when the target surface is rigid and the contact surface is flexible, or both surfaces are flexible). This is because the underlying finite elements for flexible bodies excite higher frequencies, which can make the time integration scheme unstable unless some numerical damping is used. For rigid bodies undergoing only translation motion and impact, numerical damping is generally not needed; however, when rigid bodies are undergoing large rotations, a small amount of numerical damping is necessary to keep the time integration scheme from becoming unstable. Non Linear explicit finite element analyses enable prediction of damage caused by the foreign object impact without the need for costly and time consuming experiments. This ability is particularly useful in the certification phase of the design process, in which the compliance with certification requirements has to be demonstrated. Numerical

methods and techniques are therefore still being improved in order to enhance the accuracy of bird impact simulations and, consequently, reduce the requirements for experiments.

The four main modeling methods that are currently available are: the Lagrangian mesh, the Eulerian mesh, the Arbitrary Lagrangian-Eulerian (ALE) mesh, and the Smooth Particle Hydrodynamic (SPH) method. Among these, SPH method is considered for result analysis.

Among the three modeling methods mentioned earlier in that the SPH method is presented along with a brief parametric study of the factors influencing the fluid-structure interaction. They are compared and evaluated with respect to the theoretical information.

SPH FORMULATION

The Smooth Particle Hydrodynamics is a Lagrangian mesh less technique and was developed by Monaghan in the late 1970˝s for astrophysics problems with application to hypervelocity impacts (~10 km/s) where the material shatters upon impact. It is both effective and accurate at modelling material deformation as well as adaptable in terms of specific material models and besides to solve computational fluid dynamic problems, it can be also applied for continuum mechanics problems with large deformations, as crash simulations. In the SPH formulation the fluid is represented as a set of moving particles, each one representing an interpolation point, where all the fluid properties are known.

The influence of each particle is established inside of a sphere of radius of 2h, called support domain Ωh, where h is the smoothing length, as shown in the figure 3.4.

The smoothing length of every particle changes with the time. When particles separate the smoothing length increases, while when they come close to each other, the smoothing length decreases accordingly.

It is necessary to keep enough particles in the neighbourhood to validate the approximation of continuum variables. Because of the grid less nature of the methodology, the SPH does not suffer from the usual disadvantage relative to mesh tangling in large deformation problems, like a pure Lagrangian formulation, and uses fewer elements than the ALE method, avoids the material interface problems associated with it.

The rest of the paper is organized as follow: The next section covers the theory related to bird strike. The results obtained with the available models are presented. The conclusions are drawn in the last section.

This paper aims at summarizing the steps involved in creating the bird model. It describes the theory of the bird strike and provides a sample of the available experimental data. Then a demonstration is given as to how to evaluate a bird model based on the following criteria: Variation of Kinetic and Internal Energy and momentums with time for all bird shapes.

THEORY OF BIRD STRIKE

A bird undergoing impact at high velocity behaves as a highly deformable projectile where the yield stress is much lower than the sustained stress. Accordingly, the impact can be qualified as a hydrodynamic impact. That, and the fact that the density of flesh is generally close to the density of water, makes it possible for a bird to be considered as a lump of water hitting a target. This is the main assumption leading to the understanding of the behaviour of a bird.

P-alpha EOS

In the p-α model[2, 3] the compaction function defines the distension in terms of pressure, which conveniently expresses exactly what is measured in laboratory crush experiments. However, due to the interdependence of pressure and distension, implementation of the p-α model in a hydrocode often requires iterative subcycling to find both simultaneously [4].

EOS of water and air

Additional useful information resulting from associating the bird to the water is the equation of state (EOS) used to describe the pressure-density (*p*-*ρ*) relationship in the bird medium. A few equations are available and the one most commonly used for the water-bird is a polynomial of degree 3 [5, 6]. This polynomial EOS for the bird model corresponds to a hydrodynamic, isotropic, and non-viscous constitutive law and is given as follows:

$$p = C_0 + C_1\mu + C_2\mu^2 + C3\mu^3 \quad \text{.....(1)}$$

Where μ is given by $\mu=\rho/\rho_0-1$ and represents the change in density during the impact. This polynomial equation of state for the bird model corresponds to a hydrodynamic, isotropic, and non-viscous constitutive law.

The coefficients are given by expressions based on the initial density ρ_o, the speed of sound in water and an experimental constant *k*. The expressions are:

C_0-Initial Equilibrium Pressure, Considered to be Negligible

$$C_1 = \rho_0 c_0^2$$

$$C_2 = (2k-1)C_1 \quad \text{.....(2)}$$

$$C_3 = (k-1)(3k-1)C_1$$

ISSN: 2277-9655
(I2OR), Publication Impact Factor: 3.785

where is: ρ_0 - density of the medium (for the water $\rho_{0,w}$ = 1000 kg/m^3 and for the air $\rho_{0,a}$ = 1.225 kg/m^3), c_0 - speed of the sound in the medium (for the water $c_{0,w}$ = 1483 m/s and for the air $c_{0,a}$ = 342 m/s) and k - experimental constant (for the water k_w = 2.0 and for the air k_a = 1.03).

EOS of porous material

The EOS of porous material is based on the thermodynamic equation that describes the state of matter under a given set of physical conditions. It is a constitutive equation that provides a mathematical relationship between two or more state functions such as the temperature T, the Volume V or density, pressure and internal energy:

$$p = p(\rho, E) = p(V, E) = p(\rho, T) = V,T) \quad \text{.....(3)}$$

Further development of the theory for porous medium requires the elastic bulk modulus and the sound speed of porous to be defined[7]. The sound speed is calculated assuming:

$$c_{por} = (1-z)^m c_{o,w} + z c_{o,a} \quad \text{.....(4)}$$

The diagram in Fig.1 illustrates the developed distribution for the exponent values m =1.

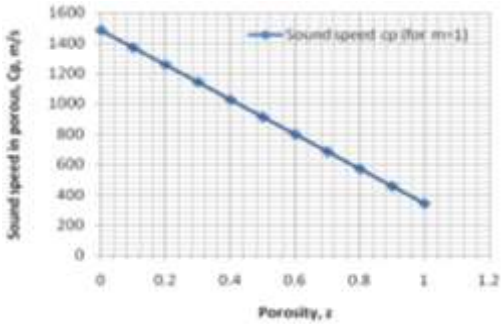

Figure: ***1. Sound speed distribution depending on porosity.***

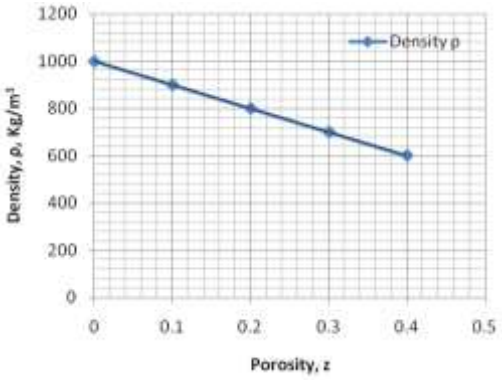

Fig. 2. Density distribution depending on porosity.

FEM MODELING

Bird model

For a bird material a homogeneous mixture of water and air was used. The porosity (volume presence of the air) varied from z = 0.0 to z = 0.4. The effect of porosity with the P-alpha EOS for porous material was investigated. The appropriate mechanical parameters of the water and the water-air mixture depending on porosity are given in Table 1.

Table 1. Mechanical parameters of the water and the water-air mixture

Porosity z	Density ρ	Sound speed c_p (for m=1)	Bulk modulus K (for m=1)
--	kg/m^3	m/s	MPa
0.0	1000.0	1483	2200
0.1	900.12	1368	1668
0.2	800.25	1256	1260
0.3	700.37	1142	907
0.4	600.49	1026	632

For the purpose of this research, two typical *bird shapes* generally used in the bird strike analysis, a flat and a hemispherical cylinder were considered. In each case, the height and the diameter of the bird was assumed to be 200 mm and 100 mm, respectively. The length-to-diameter ratio of 2 for each bird shape was identical.

Two types of the numerical models of body shapes based on the SPH particles distributions along the symmetry axis are presented in Fig.3.

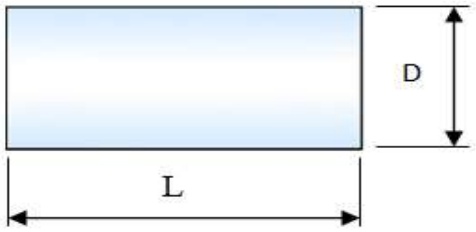

Fig. (a) Cylindrical

ISSN: 2277-9655
(I2OR), Publication Impact Factor: 3.785

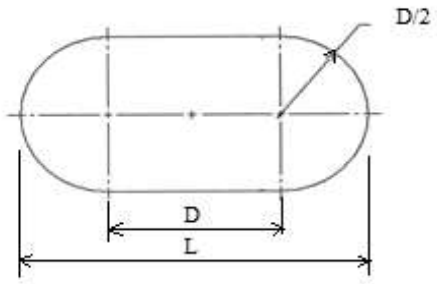

Figure: (b).Cylindrical with hemispherical ends.

Figure:3.Different substitute bird impactor geometries.

Target model

The target structure was considered as composite square plate (Epoxy_Carbon_UD) with the dimensions of 700 × 700 mm and the thickness 14mm was modeled as 8 prepregs of each 0.5mm thick and 10mm Honeycomb placed symmetrically in between the prepregs. All degrees of freedom of the target structure of 4 edges were constrained.

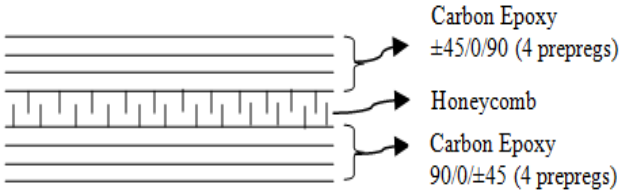

Figure:4. Sandwich structure of a composite

The target flexibility was introduced into the analysis, and the inherent coupling between the impact loads and the target deflection was explored.

The appropriate mechanical parameters of the Epoxy_Carbon_UD are

Density ρ=1490Kg/m^3

Orthotropic elastic limits:

E_x=1.21x10^{11} N/m^2
E_y=8.6x10^9 N/m^2
E_z=8.6x10^9 N/m^2
μ_{xy}=0.27
μ_{xy}=0.4
μ_{xy}=0.27
G_{xy}=4.7x10^9 N/m^2
G_{yz}=3.1x10^9 N/m^2
G_{xz}=4.7x10^9 N/m^2

Orthotropic stress limits:

- Tensile stresses:

σ_x =2.231x10^9 N/m^2
σ_y =2.9x10^7 N/m^2
σ_z =2.9x10^7 N/m^2

- Compressive stresses:

σ_x =1.082x10^9 N/m^2
σ_y =1x10^8 N/m^2
σ_z =1x10^8 N/m^2

- Shear stresses:

τ_{xy}=6x10^7 N/m^2
τ_{yz}=3.2x10^7 N/m^2
τ_{xz}=6x10^7 N/m^2

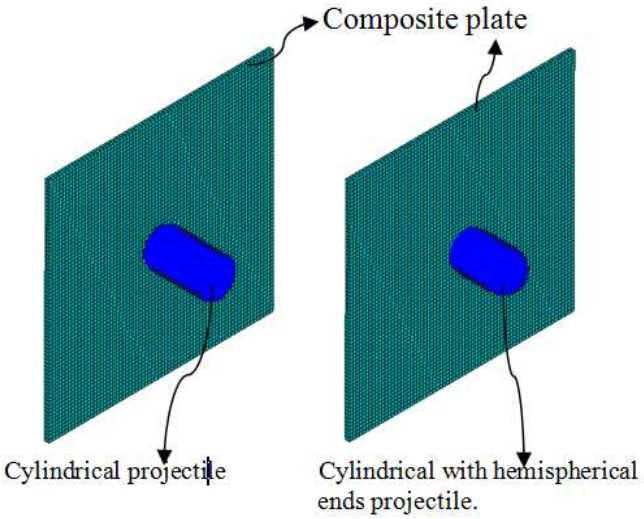

Figure: 5. Lagrangian model of a Composite target and an SPH model of a cylindrical and Cylindrical with hemispherical ends projectile

RESULTS AND DISCUSSION

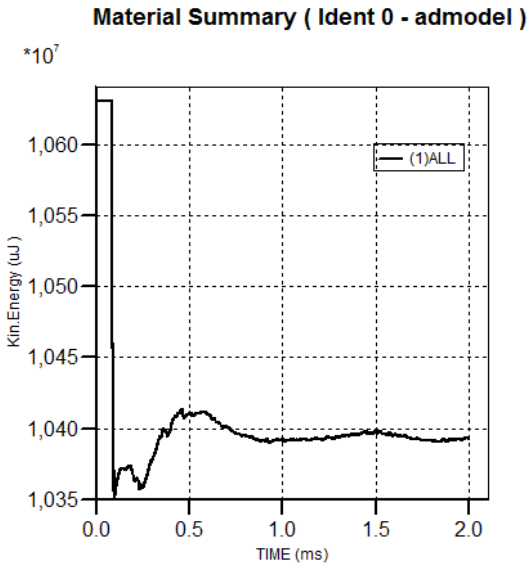

Figure: a) Cylindrical

ISSN: 2277-9655
(I2OR), Publication Impact Factor: 3.785

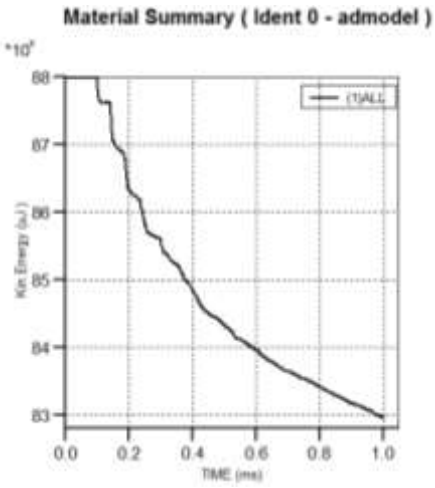

Figure: b) Cylindrical with hemispherical ends.
Fig.6. Comparison of Kinetic Energy with time of cylindrical and Cylindrical with hemispherical ends projectile with porosity z=0.0 and impact velocity V_{im}=116m/s.

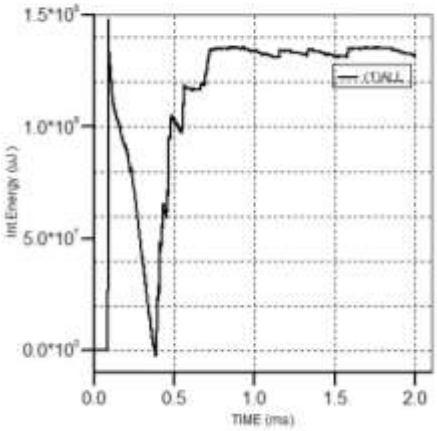

Figure: a) Cylindrical

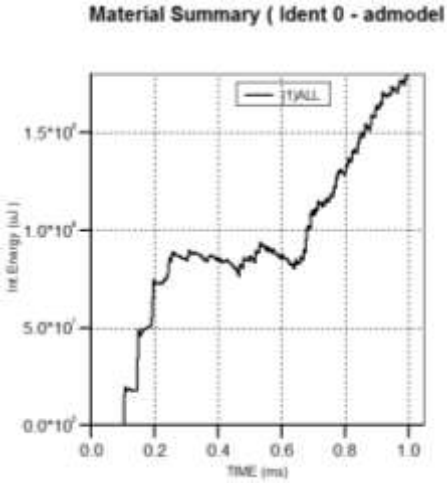

Figure: b) Cylindrical with hemispherical ends.

Figure:7.Comparison of Internal Energy with time absorbed by target structure impacted by cylindrical and Cylindrical with hemispherical ends projectile with porosity z=0.0 and impact velocity V_{im}=116m/s.

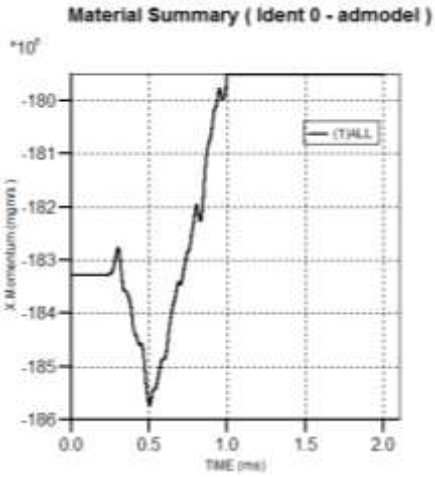

Figure: a) Cylindrical

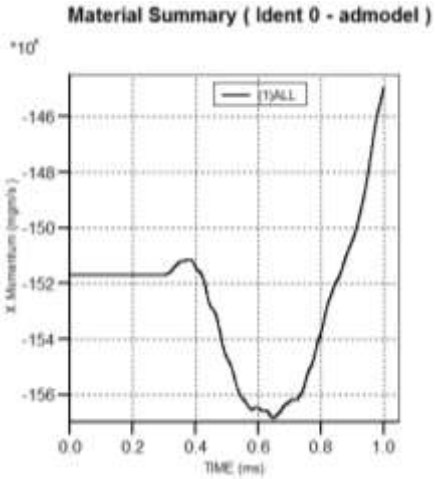

Figure: b) Cylindrical with hemispherical ends.
Figure:8. Comparison of Momentums of a cylindrical and Cylindrical with hemispherical ends projectile with porosity z=0.0 and impact velocity V_{im}=116m/s.

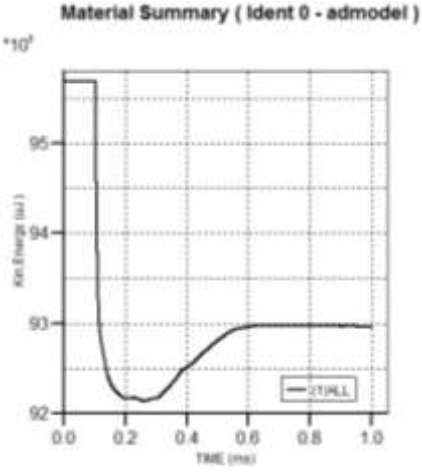

Figure: a) Cylindrical

ISSN: 2277-9655
(I2OR), Publication Impact Factor: 3.785

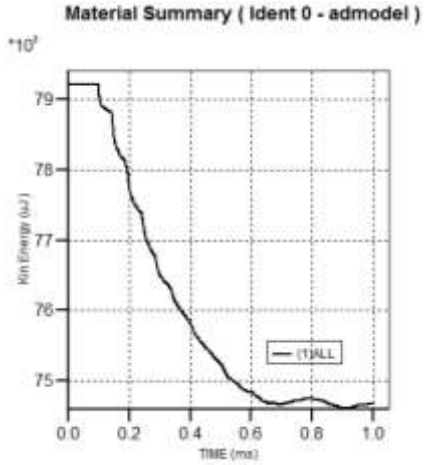

Figure: b)Cylindrical with hemispherical ends.

Figure:9. Comparison of Kinetic Energy with time of cylindrical and Cylindrical with hemispherical ends projectile with porosity z=0.1 and impact velocity V_{im}=116m/s.

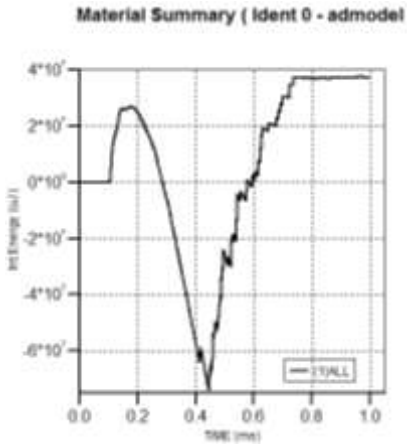

Figure: a) Cylindrical

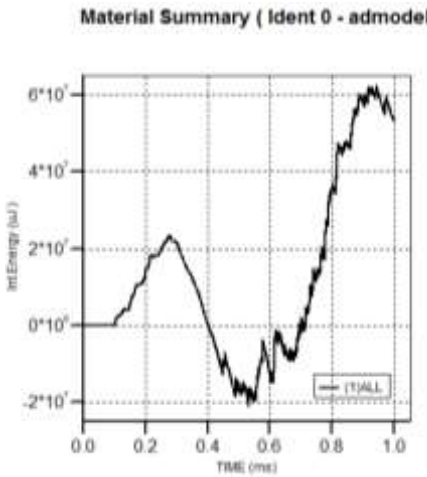

Figure: b) Cylindrical with hemispherical ends.

Figure: 10. Comparison of Internal Energy with time absorbed by target structure impacted by cylindrical and Cylindrical with hemispherical ends projectile with porosity z=0.1 and impact velocity V_{im}=116m/s.

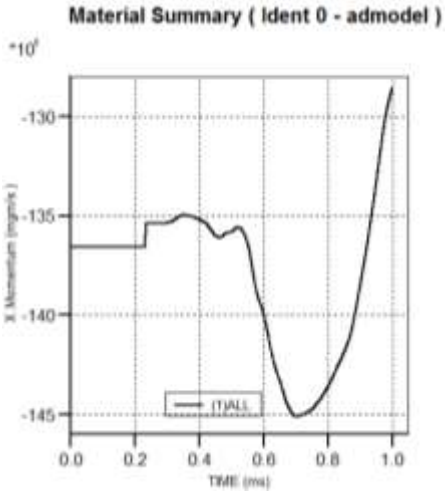

Figure: a) Cylindrical

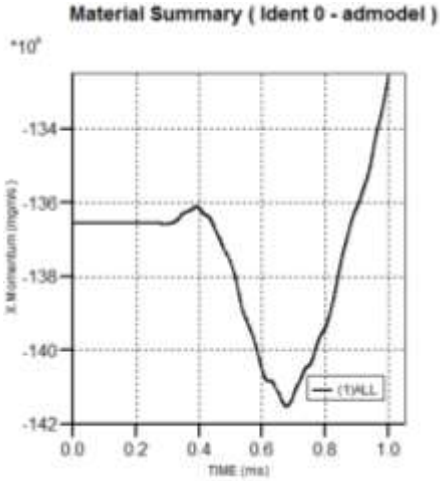

Figure: b) Cylindrical with hemispherical ends.

Figure: 11. Comparision of Momentums of a cylindrical and Cylindrical with hemispherical ends projectile with porosity z=0.1 and impact velocity

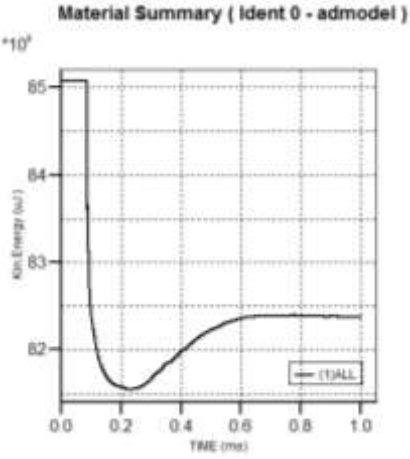

Figure: a) Cylindrical

ISSN: 2277-9655
(I2OR), Publication Impact Factor: 3.785

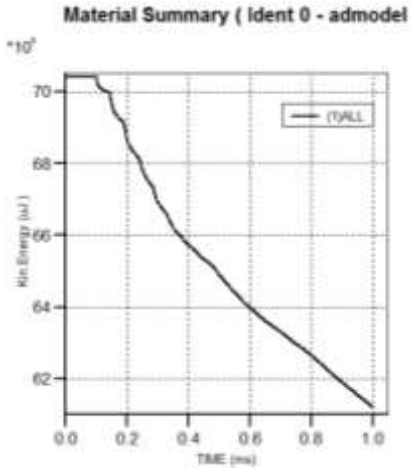

Figure:b) Cylindrical with hemispherical ends.

Figure:12. Comparison of Kinetic Energy with time of cylindrical and Cylindrical with hemispherical ends projectile with porosity z=0.2 and impact velocity V_{im}=116m/s.

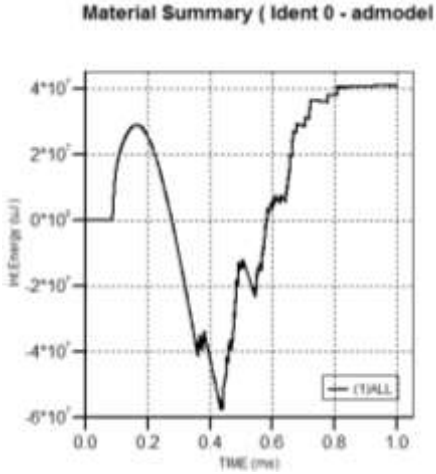

Figure: a) Cylindrical

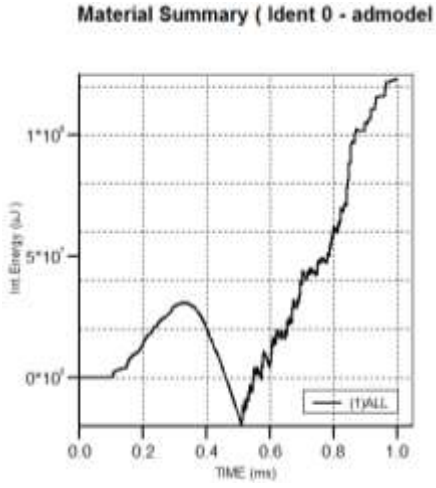

Figure: b) Cylindrical with hemispherical ends.

Figure:13. Comparison of Internal Energy with time absorbed by target structure impacted by cylindrical and Cylindrical with hemispherical ends projectile with porosity z=0.2 and impact velocity V_{im}=116m/s.

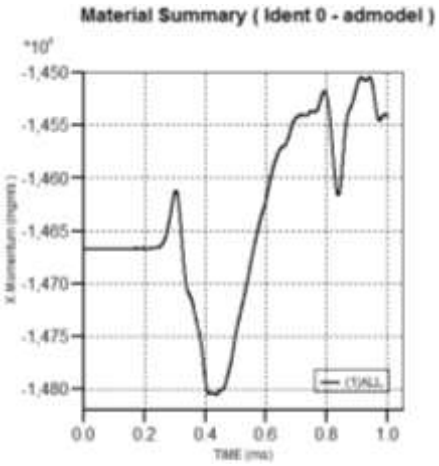

Figure: a) Cylindrical

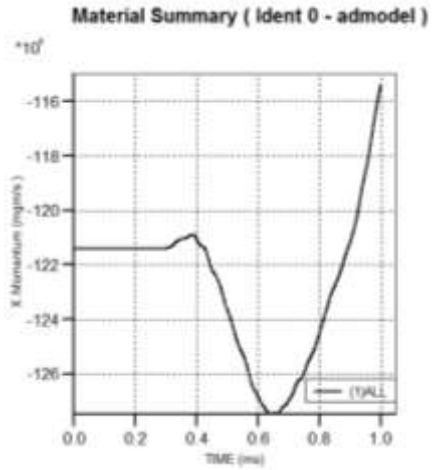

Figure: b) Cylindrical with hemispherical ends

Fig. 14. Comparison of Momentums of a cylindrical and Cylindrical with hemispherical ends projectile with porosity z=0.2 and impact velocity V_{im}=116m/s.

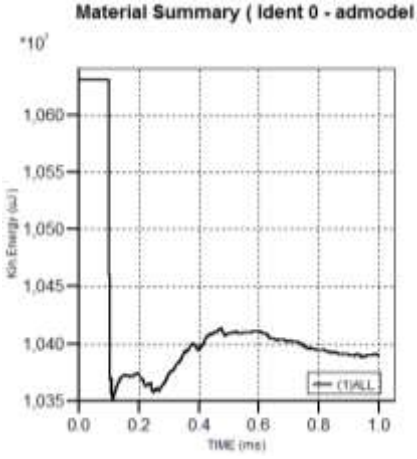

Figure: a) Cylindrical

ISSN: 2277-9655
(I2OR), Publication Impact Factor: 3.785

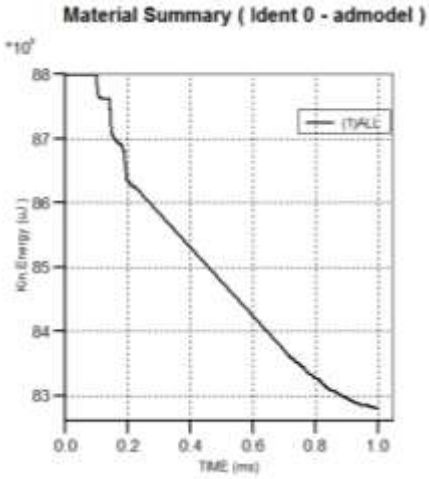

Figure: b) Cylindrical with hemispherical ends.

Figure:15. Comparison of Kinetic Energy with time of cylindrical and Cylindrical with hemispherical ends projectile with porosity z=0.3 and impact velocity V_{im}=116m/s

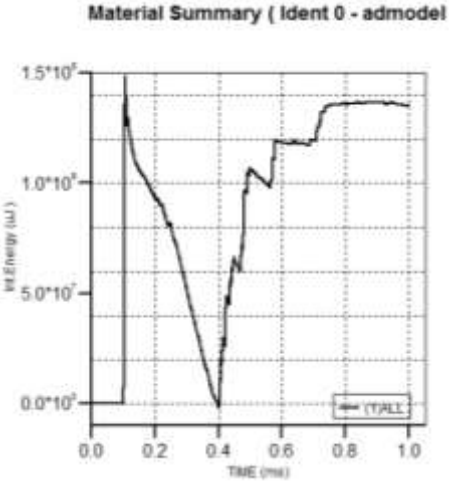

Figure: a) Cylindrical

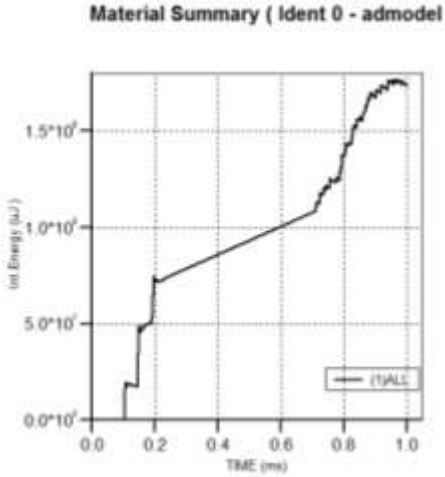

Figure: b) Cylindrical with hemispherical ends.

Fig.16. Comparison of Internal Energy with time absorbed by target structure impacted by cylindrical and Cylindrical with hemispherical ends projectile with porosity z=0.3 and impact velocity V_{im}=116m/s.

Figure: a) Cylindrical

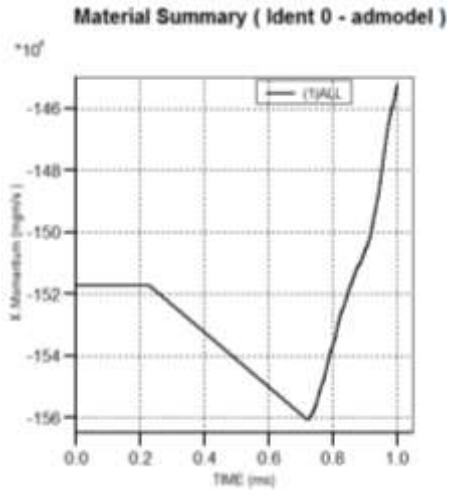

Figure: b) Cylindrical with hemispherical ends.
Fig.17.Comparison of Momentums of a cylindrical and Cylindrical with hemispherical ends projectile with porosity z=0.3 and impact velocity V_{im}=116m/s.

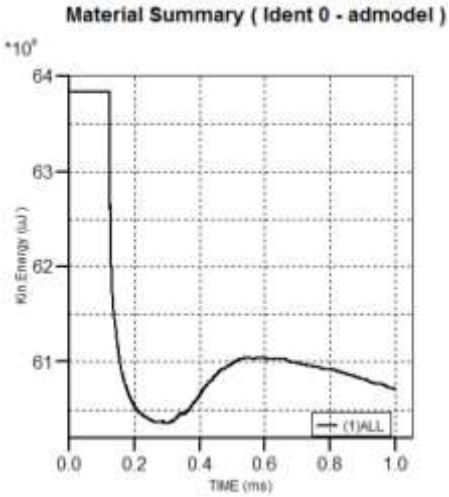

Figure: a) Cylindrical

ISSN: 2277-9655
(I2OR), Publication Impact Factor: 3.785

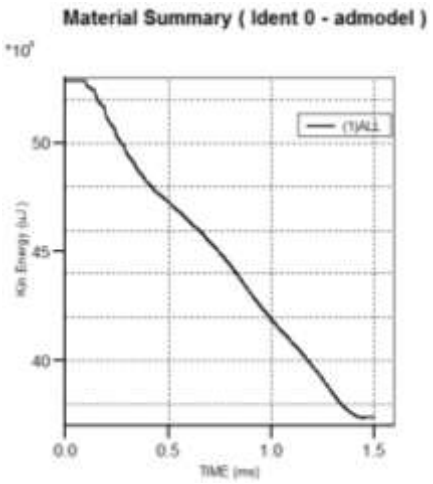

Figure: b) Cylindrical with hemispherical ends

Fig.18. Comparison of Kinetic Energy with time of cylindrical and Cylindrical with hemispherical ends projectile with porosity z=0.4 and impact velocity V_{im}=116m/s.

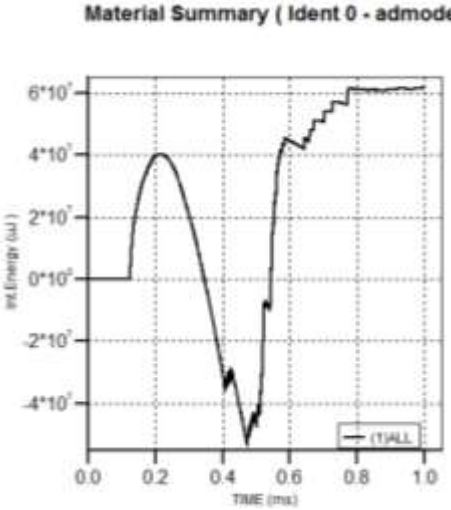

Figure: a) Cylindrical

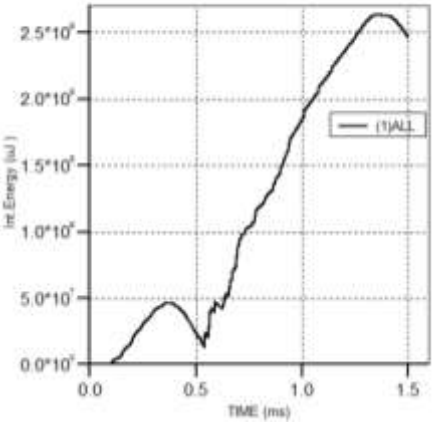

Figure: b) Cylindrical with hemispherical ends

Figure:19. Comparison of Internal Energy with time absorbed by target structure impacted by cylindrical and Cylindrical with hemispherical ends projectile with porosity z=0.4 and impact velocity V_{im}=116m/s.

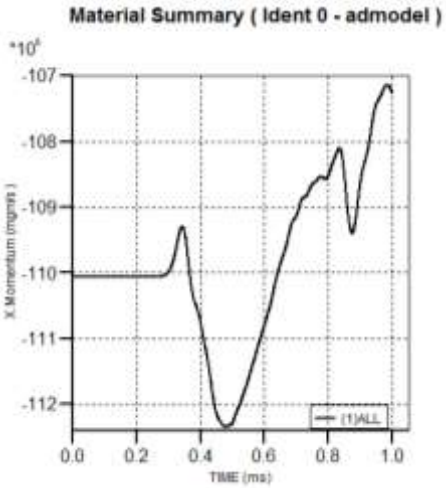

Figure:a) Cylindrical

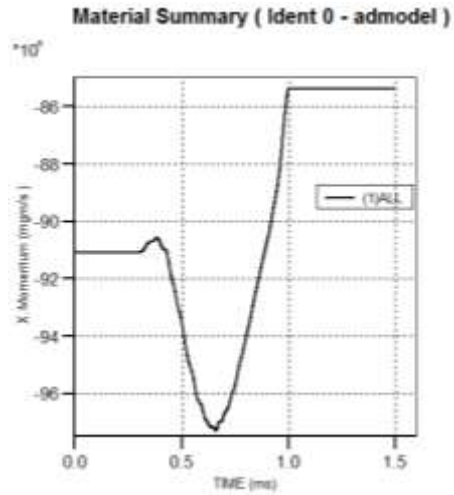

Figure:b) Cylindrical with hemispherical ends.

Fig.20. Comparison of Momentums of a cylindrical and Cylindrical with hemispherical ends projectile with porosity z=0.4 and impact velocity V_{im}=116m/s.

Comparing the results of the numerical simulations of the bird impact on the Composite target, for a flat cylinder and a hemispherical cylinder shape of the bird body, gives the following:

-Maximum Kinetic Energy distributions (Figures 6, 9, 12, 15 and 18) comparing the flat cylinder impact shows 17.29% higher Kinetic Energy values than in the case of the hemispherical ended cylinder impact;

-Internal Energy absorbed by the Composite plate (Figures 7, 10, 13, 16 and 19) comparing the flat cylinder impact shows 14.28% lower values than in the case of the hemispherical ended cylinder impact; and

-Momentums of the projectile (Figures 8, 11, 14, 17 and 20) comparing the flat cylinder impact shows 17.93% higher values than in the case of the hemispherical ended cylinder impact.

CONCLUSIONS

A homogeneous water-air mixture was used for the bird material and the equation for the elastic bulk modulus and the sound speed of porous medium depending on porosity was involved in the analysis.

Finite element numerical simulations of the bird impact were carried out by the SPH method to represent the bird body. Based on the mechanical parameters, determined by the proposed equation, the effect of porosity with the P-alpha EOS for porous materials was tested.

The numerical simulation of various cases of the bird impact including the variation of bird material density, shape and impact velocity, and target plate parameters was successfully performed.

Regarding the shape, it can be seen that the predicted energies and momentums associated with two bird shapes, among these, the cylindrical with hemispherical ended bird shape with porosities 0.3 and 0.4 results gives very nearer to experimental values[6].

REFERENCES

[1]Federal Aviation Administration, *Policy for Bird Strike*, (U.S. Department of Transportation, 2002)

[2]Herrmann W. Constitutive Equation for the Dynamic Compaction of Ductile Porous Materials. *Journal of Applied Physics*, 1969; **40** (6), 2490-2499.

[3]Carroll MM, Holt AC. Static and Dynamic Pore-Collapse Relations for Ductile Porous Materials. *Journal of Applied Physics*, 1972; **43**(4), 1626-1636.

[4]Kerley GI. 1992. Sandia National Lab Report, SAND 92-0553.

[5]IVANČEVIĆ,D., SMOJVER,I.: *Hybrid approach in bird strike damage prediction on aeronautical composite structures*, Composite Structures, 2011, 94, 1, pp.15-23.

[6]NIZAMPATMAN,L.S.: *Models and methods for bird strike load predictions*, PhD Dissertation, Faculty of Graduate School, Wichita State University, USA, (2007).

[7]Marinko Ugrčić, Application of the Hydrodynamic Theory and the Finite Element Method in the Analysis of Bird Strike in a Flat Barrier, Scientific Technical Review, 2012,Vol.62, No.3-4,pp.28-37.